Supplement to: The strengths and limitations of using biolayer interferometry to monitor equilibrium titrations of biomolecules.

Chamitha J. Weeramange, Max S. Fairlamb, Dipika Singh, Aron W. Fenton and Liskin Swint-Kruse

Department of Biochemistry and Molecular Biology, The University of Kansas Medical Center, Kansas City, KS.

Supplementary Methods: Protein Purification and validation

LacI and LLhF

Wild-type tetrameric LacI was purified according to Swint-Kruse, et al (1). Protein concentration was determined from the A_{280} for wild-type LacI, using an extinction coefficient of 0.6 $([mg/ml]\bullet cm)^{-1}$ (2; 3). For both LacI and LLhF, the concentration of active repressor protein was confirmed using filter binding assays in the stoichiometric binding regime (with the DNA concentration at a concentration at least ten times greater than K_d) (4).

To express LLhF protein, the gene encoding LLhF (5) was substituted for the gene encoding LacI on the high copy pLS1 plasmid (6). This plasmid uses the *lacI*^{q} promoter for constitutive gene expression and carries an ampicillin resistance gene. The plasmid was transformed into the *E.coli* B *omp*T, *hsdS*$_B$($r_B^- m_B^-$)$^-$, *gal, dcm, lac* cells (strain name BLIM (7)) and grown in 6 L 2xYT media overnight. Pelleted cells were resuspended in ~50 mL "breaking buffer" (0.2 M Tris-HCl, 0.2 M KCl, 0.01 M $Mg(CH_3COO)_2$, 1 mM DTT, 5% glucose, pH 7.6) with 20 mg lysozyme and a crushed Pierce Protease Inhibitor Tab (Thermo Scientific, Rockford, IL) and frozen at -20°C until further use. All subsequent purification steps were carried out on ice or at 4°C. Cell lysis was accomplished by thawing the cell pellet on ice with breaking buffer added to a final volume of 150 mL and another crushed protease tab. At this step, the addition of 130 mg extra lysozyme was critical for chaperoning the LLhF through ammonium sulfate precipitation, which was an unexpected activity of lysozyme. After lysis, 240 µL of 80 mg/ml DNase I from bovine pancreas (Roche Diagnostics, Mannheim, Germany) was added along with $MgCl_2$ (Fisher Scientific, UK) to a final concentration of 30 mM. The crude cell extract was cleared by centrifugation at 8,000 rpm for 50 min at 4°C prior to 23% ammonium sulfate precipitation (Fisher Scientific, Fair Lawn, NJ).

After precipitation, the pellet was gently resuspended in 50 mL cold 0.05 M KP buffer and dialyzed in regenerated cellulose Fisher brand Dialysis Tubing (MWCO 12,000-14,000) against 1 L of cold 0.05 M KP buffer for 30 minutes, with three buffer changes. (KP buffer comprises potassium phosphate at the indicated molarity, 5% glucose, 0.3 mM DTT, pH 7.5.) The dialysate was cleared by centrifugation and loaded onto a phosphocellulose column (Whatman P11) that was pre-equilibrated in 0.05 M KP buffer. A gradient of 0.05 M to 0.2 M KP buffer was used to elute the protein. By SDS-PAGE, small amounts of FruK were also observed in the final, purified LLhF. However, since a strong signal could be detected for LLhF binding to purified FruK (Figure 8 in the main text), the trace contaminants must be well-below saturation levels. Purified LLhF was aliquoted and stored at -80°C. Protein concentration was determined by Bradford assays (Bio-Rad Laboratories, Inc. Hercules, CA) and was generally 0.20 mg/ml ($6x10^{-6}$M).

Fructose-1-kinase (FruK)

The third protein used in this project is *E. coli* fructose-1-kinase (FruK). This previously-unidentified protein was first noted in pull-down assays of *E. coli* crude cell extracts, which used immobilized *lac* operator DNA to assess LLhF-expression levels prior to *in vivo* repression as-

says (5). In the pull-down results, we noted that LLhF bound a hetero-protein (see Supplementary Figure 1 in reference (5)). These two bands are best observed using a Phast-gel 10-15% gradient, (GE Healthcare, Piscataway, NJ; catalogue #: 17-0540-01); to date, the resolution of other gels has been insufficient to resolve them. To confirm the identity of LLhF in the top band and identify the second band as FruK, the two bands were excised from the gel and subjected to trypsin digestion. They were then submitted for mass spectrometry analyses at the Mass Spectrometry Core Laboratory at KUMC. Results were analyzed using the Sequest algorithm to search an *E. coli* protein database derived from the NCBI-NR repository on February 2, 2011 (Supplementary Table I). In these analyses, trypsin specificity was requested with a maximum of two missed cleavages. Oxidation of methionine, deamidation of asparagine and glutamine, and carboxymethylation of cysteine (defined as a fixed modification) were defined as variable modifications. Statistical criteria for peptide identification included: a minimum XC of 1.8, 2.5 or 3.5 for a peptide ion with a charge of 1, 2, or 3, respectively, a minimum Delta Cn of 0.01, and a probability of 0.001. For protein identification, a minimum of two unique peptides was required.

To purify FruK protein, we obtained the FruK-pET-3a plasmid from Schaftingen and co-workers and adapted their purification protocol (8). Briefly, the expression plasmid was transformed into F–, *omp*T, *hsd*S_B (r_B–, m_B–), *dcm*, *gal*, λ(DE3), pLysS, Cm^r.cells (strain name BL21). These cells were used to inoculate 3 mL aliquots of 2xYT media and grown overnight at 37°C. Six mL of these cultures were subsequently used to inoculate each of three 2 L flasks containing 1 L M9 media (211 mM Na_2HPO_4, 110 mM KH_2PO_4, 93.4 mM NH_4Cl, 42.8 mM NaCl,135 µM $CaCl_2$, 1 mM $MgSO_4 \bullet 7H_2O$, 0.2% glucose, 50 ug/ml ampicillin, 0.00005% vitamin B1, 0.1% casamino acids, pH 7.4). Each 1 L of M9 media was grown for 3-5 hours at 37°C until OD_{600} reached 0.6, then induced with 1 mM IPTG. Induced cultures were incubated at 22°C with shaking at 220 rpm for an additional 44-45 hours.

FruK-expressing cells were pelleted at 7,000 rpm for 15 min and resuspended in 50 mL of FruK breaking buffer (20 mM potassium phosphate, 5 mM EDTA, 1 mg/mL lysozyme, 1 Pierce Protease Inhibitor Tablet (Thermo Scientific, Rockford, IL), 1 mM DTT, pH 7.4). The crude cell lysate was cleared by centrifugation and protein purification proceeded as described (8) using ammonium sulfate precipitations followed by a Sephadex G25 column for the desalting step and DEAE-sepharose for the anion exchange step. The latter was accomplished with two gradient-elution steps comprising (i) 20-250 mM KCl in Buffer A (20 mM Hepes, 20 mM KCl, ½ protease tablet (Thermo Scientific), 10% glycerol) and (ii) 250-500 mM KCl in Buffer A. Alternatively, instead of the G25 column, we decreased the ionic strength of the resuspended FruK by diluting the ammonium sulfate resuspension 1:5 with 20 mM KCl Buffer A and then reducing the supernatant volume by half with a Vivaspin MWCO 10 kDa concentrator (Sartorius Stedim Lab Ltd, Stonehouse, UK) and centrifugation with an HB-6 at 5500 rpm for 12-15 minutes at 4 ^{0}C. We found the latter performed better in the anion exchange step. After anion exchange, the FruK-containing fractions were brought to 20% glycerol prior to freezing at -80°C. Protein concentration was determined by Bradford assays (Bio-Rad Laboratories, Inc. Hercules, CA). Glycerol is a key buffer component. If this osmolyte was removed by dialysis, FruK enzymatic activity decayed over the course of 30 min – 1 hour.

Prior to LLhF-FruK binding experiments, we verified the catalytic activity of purified FruK and assessed its activity in buffers used for binding assays. FruK catalyzes the reaction (9):

$$\text{F-1-P + ATP} \xrightleftharpoons{\textbf{FruK}} \text{F-1,6-BP + ADP} \qquad \text{[Equation S1]}$$

To confirm the catalytic activity of purified FruK, we first replicated the published assay that coupled the FruK reaction to those of aldolase C, triose phosphate isomerase, and glycerophosphate dehydrogenase, ultimately measuring the 340 nm absorbance of NADH (8). From this, we used the Michaelis-Menten equation to determine a K_m value of 0.4 mM, which is in reasonable agreement with the previously published value of 0.13 mM (8).

However, we found that the commercial aldolase used as a coupling enzyme had inconsistencies and sometimes quite high activity towards F-1-P. Therefore, we devised a new assay by coupling the FruK reaction to that of pyruvate kinase from rabbit muscle (Roche, Mannheim, Germany) and lactate dehydrogenase (Calzyme Laboratories, San Luis Obispo, CA).

$$\text{PEP + ADP} \xrightleftharpoons{\textbf{PYK}} \text{pyruvate + ATP} \qquad \text{[Equation S2]}$$

$$\text{pyruvate + NADH} \xrightleftharpoons{\textbf{LDH}} \text{lactate + NAD}^+ \qquad \text{[Equation S3]}$$

Assays used 5.23 U/ml lactate dehydrogenase and 10 mg/ml pyruvate kinase, following the example of pyruvate kinase studies (*e.g.* (10)). Other reagents included phosphoenolpyruvate (PEP; 10 mM; Chem-Impex, International, Wood Dale, IL), ATP (Chem-Impex; 3mM), NADH (Sigma Chemical Co; 0.18 mM), and F-1-P. The reaction rate for FruK was monitored by the depletion of NADH at 340 nm in a SPECTRAmax PLUS 384 at 30°C using a UV-Star flat bottom 96-well plate (Greiner Bio-One, Monroe, NC).

Reactions were initiated by the addition of ATP. Initial velocities were determined as a function of F-1-P concentration and used to estimate values of K_m with the program GraphPad Prism 5 (GraphPad Software Inc., La Jolla, CA) and the Michaelis-Menten equation. Representative results are shown in Supplementary Figure 10, below. From assays performed with several preparations of FruK, we found that K_m for F-1-P was in the range of 0.5-2 mM. In the absence of substrate ATP, no activity was detected, which showed the F-1-P activity was due to FruK and not to the coupling enzymes. Based on these results, we concluded that our preparation of FruK was similar to those previously reported in the literature.

We used the new enzymatic assay to compare FruK activities in two different buffers: (i) that of Viega de Cunha and colleagues (8) (20 mM Hepes, pH 7.1, 5 mM $MgCl_2$, and 50 mM KCl, with 2.5 mM ATP and 0.15 mM NADH) in order to compare to published results and (ii) that used for pyruvate kinase assays (10) ("PYK buffer": 50 mM Hepes, pH 7.0, 5 mM $MgCl_2$, and

50 mM KCl, with 3 mM ATP and 0.335 mM NADH), which is more similar to DNA binding buffer used in filter binding assays. We observed no noticeable difference in enzyme activity between the two buffers and therefore we used the PYK buffer for LLhF-FruK binding assays.

For BLI assays, FruK was diluted ~1:5 (to $8x10^{-3}$ mg/ml) with FruK exchange buffer (20 mM Hepes, 40 mM KCl, 1mM EDTA, 20% glycerol, 0.3 mM DTT, pH 7.0) and concentrated ~15-fold in VivaSpin concentrators with a MWCO of 10,000 Da. This was repeated two more times prior to binding experiments. This procedure was carried out to remove the small molecule contaminant previously reported (11).

Supplementary Table I. Mass spectrometry identification of LLhF[a] and FruK[b]

		MH+	z	P(pep)	XC	DeltaCN
Upper gel band						
FruR [Escherichia coli]				**2.49e-10**	**130.32**	
471[c]	R.EHNYHPNAVAAGLR.A	1549.67534	2	2.55E-06	2.58	0.51
1163	R.EAAAQLFEK.W	1007.12198	1	4.77E-05	2.14	0.20
1384	R.EVHFLYANSYER.E	1528.64967	1	3.04E-08	3.13	0.51
1899	R.GYQLLIAC#SEDQPDNEM*R.C	2156.33989	2	2.49E-10	4.59	0.64
2176	R.GYQLLIAC#SEDQPDNEMR.C	2140.34049	2	9.57E-10	6.18	0.68
2322	R.EHFTSVVGADQDDAEM*LAEELRK.F	2607.79231	3	1.95E-06	4.50	0.57
2399	R.EHFTSVVGADQDDAEMLAEELRK.F	2591.79291	3	4.85E-09	5.21	0.56
2472	R.QVDAIIVSTSLPPEHPFYQR.W	2298.58241	2	2.76E-09	4.03	0.58
2491	R.EHFTSVVGADQDDAEM*LAEELR.K	2479.61940	2	2.27E-06	5.71	0.64
2809	R.EHFTSVVGADQDDAEMLAEELR.K	2463.62000	2	4.55E-10	6.45	0.70
3041	R.VLEIVLASLDEPR.K	1454.69359	2	3.40E-08	2.71	0.46
3222	R.SIGLVIPDLENTSYTR.I	1778.98434	2	1.61E-08	3.02	0.41
3942	R.WANDPFPIVALDR.A	1514.70927	2	8.86E-05	2.70	0.43
truncated LacI repressor [Escherichia coli]				**1.14E-11**	**60.24**	
245	R.VVNQASHVSAK.T	1140.27477	2	6.98E-09	2.60	0.52
1328	R.EKVEAAM*AELNYIPNR.V	1865.10071	2	2.22E-08	4.14	0.55
1377	K.VEAAM*AELNYIPNR.V	1607.81325	2	3.87E-08	4.16	0.53
1913	R.EKVEAAMAELNYIPNR.V	1849.10131	2	1.17E-10	4.68	0.55
1981	K.VEAAMAELNYIPNR.V	1591.81385	2	1.32E-05	3.84	0.53
3271	K.PVTLYDVAEYAGVSYQTVSR.V	2219.43569	2	1.14E-11	4.32	0.60
transcriptional repressor of the lac operon [Escherichia coli]				**6.03E-12**	**20.26**	
3158	-.MKPVTLYDVAEYAGVSYQTVSR.V	2478.80568	2	7.64E-09	5.15	0.73
3250	-.M*KPVTLYDVAEYAGVSYQTVSR.V	2494.80508	2	6.03E-12	3.86	0.66
Lower gel band						
FruK [Escherichia coli]				**1.84E-11**	**116.28**	
1222	R.RELEIWAGR.K	1130.28158	2	3.84E-05	3.00	0.20
1710	R.SQC#PC#IIFDSSR.E	1470.65648	2	2.90E-06	2.90	0.56
2016	R.LATAVAALAVSQSNVGITDR.P	1958.20580	2	5.66E-05	3.39	0.56
2236	R.LATAVAALAVSQSNVGITDRPQLAAM*M*AR.V	2960.42348	3	4.76E-08	3.54	0.54
2379	R.LATAVAALAVSQSNVGITDRPQLAAM*MAR.V	2944.42408	3	2.88E-04	4.07	0.60
2386	R.LATAVAALAVSQSNVGITDRPQLAAMM*AR.V	2944.42408	3	4.36E-06	3.92	0.53
2708	R.LATAVAALAVSQSNVGITDRPQLAAMMAR.V	2928.42468	3	3.89E-10	4.07	0.66
2925	K.LTEKDGEVTDFNFSGFEVTPADWER.F	2891.05076	3	2.01E-10	4.59	0.54
3219	R.VATITLNPAYDLVGFC#PEIER.G	2379.71699	2	5.34E-09	4.53	0.67
4050	K.DGEVTDFNFSGFEVTPADWER.F	2419.50073	2	1.84E-11	5.53	0.73
4094	K.DNQDGFQQLFSELGIANR.F	2053.17786	2	2.25E-10	3.67	0.46
4426	K.DLGIDVTVGGFLGK.D	1391.59436	2	5.91E-09	4.22	0.66

[a]**LLhF (LacI:FruR chimera) protein sequence**. In the sequence below, the LacI DNA binding domain and hinge helix are underlined; these domains are followed by the sequence of the FruR Cra regulatory domain. (FruR is also called "Cra"). Peptides identified by MS (above) are indicated in yellow on the sequence; some of these peptides overlap each other.

MKPVTLYDVA EYAGVSYQTV SRVVNQASHV SAKTREKVEA AMAELNYIPN RVAQQLAGKQ
SRSIGLVIPD LENTSYTRIA NYLERQARQR GYQLLIACSE DQPDNEMRCI EHLLQRQVDA
IIVSTSLPPE HPFYQRWAND PFPIVALDRA LDREHFTSVV GADQDDAEML AEELRKFPAE
TVLYLGALPE LSVSFLREQG FRTAWKDDPR EVHFLYANSY EREAAAQLFE KWLETHPMPQ
ALFTTSFALL QGVMDVTLRR DGKLPSDLAI ATFGDNELLD FLQCPVLAVA QRHRDVAERV
LEIVLASLDE PRKPKPGLTR IKRNLYRRGV LSRS*

[b]***E. coli* FruK protein sequence.** Peptides identified by MS (above) are indicated in yellow; some of these peptides overlap each other.

MSRRVATITL NPAYDLVGFC PEIERGEVNL VKTTGLHAAG KGINVAKVLK DLGIDVTVGG
FLGKDNQDGF QQLFSELGIA NRFQVVQGRT RINVKLTEKD GEVTDFNFSG FEVTPADWER
FVTDSLSWLG QFDMVCVSGS LPSGVSPEAF TDWMTRLRSQ CPCIIFDSSR EALVAGLKAA
PWLVKPNRRE LEIWAGRKLP EMKDVIEAAH ALREQGIAHV VISLGAEGAL WVNASGEWIA
KPPSVDVVST VGAGDSMVGG LIYGLLMRES SEHTLRLATA VAALAVSQSN VGITDRPQLA
AMMARVDLQP FN

[c]This peptide corresponds to the hinge helix in full-length, wild-type FruR and is not present in LLhF. The presence of this peptide in the LLhF sample suggests that endogenous *E.coli* FruR may also participate in the LLhF/FruK complex. All other FruR peptides found in this sample correspond to the regulatory domain, as expected. The only LacI peptides identified in this sample are those of the DNA-binding domain and hinge helix.

Supplementary Table II. Operator sequences used in BLI assays[a]

Name	Sequence
lacO^{1}	5'-/5Biosg/GCA TAT GGC AGC TTG AAT TGT GAG CGG ATA ACA ATT TTG CAG ACG-3'
lacO^{2}	5'-/5Biosg/ATG CAT GTT GTG TGG AAA TGT GAG CGA GTA ACA ACC TCA CAC AGG-3'
lacO^{3}	5'-/5Biosg/GCA TAT GGC AGC TTG AAC AGT GAG CGC AAC GCA ATT TTG CAG CGA-3'
O^{non}	5'-/5Biosg/ATG CAT GTT GTG TGG AGA CAT GCC TAG ACA TGC CTT TCA CAC AGG-3'
fruB-proximal	5'-/5Biosg/ATG CAT GTT GTG TGG TTC TTG AAA CGT TTC AGC TCA CAC AGG TCC-3'

[a]Double stranded, 45-mer oligos were used in the BLI assay; all operators were biotinylated at the 5' end of the strand shown above. The sequence for *fruB-proximal* is from (12).

Supplementary Figure 1. Biolayer Interferometry: kinetics of biomolecular interactions.

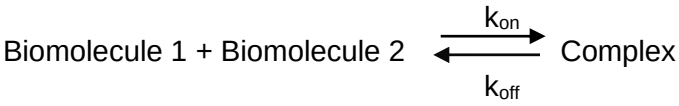

k_{on} = Association rate constant
k_{off} = Dissociation rate constant
K_d = Equilibrium binding constant

$$K_d = k_{off} / k_{on}$$

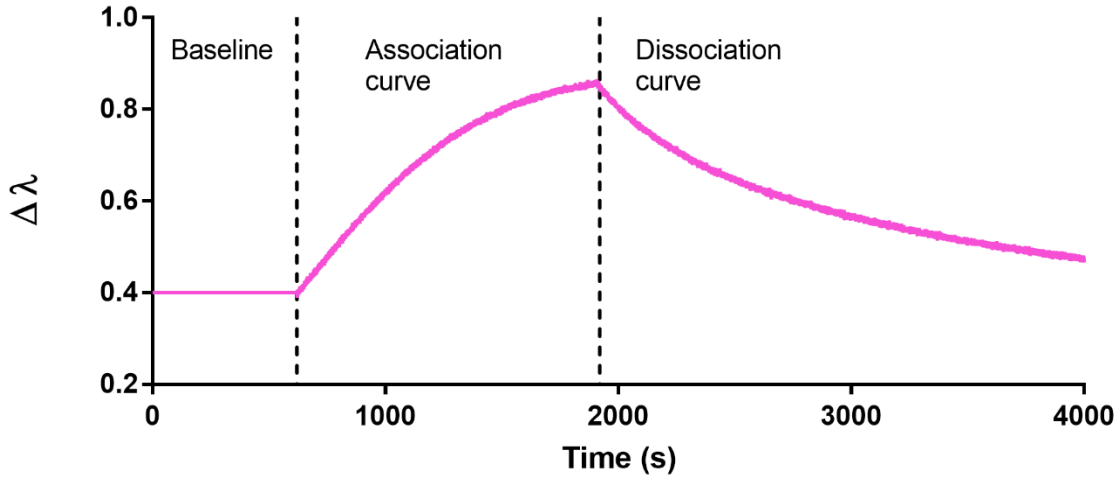

Hypothetical association and dissociation reactions monitored with biolayer interferometry ("BLI"; Δλ) as a function of time. The dashed vertical lines indicate the times when the BLI sensor tip with immobilized binding partner was moved from (left line) a starting condition to a solution containing binding partner and (right line) back to buffer. BLI was designed to monitor association and dissociation events and thereby quantify K_d from the ratio k_{off}/k_{on}. However, for the protein-DNA interactions described in this manuscript, kinetic curves could not be fit with a simple exponential equation (*e.g.* Supplementary Figures 2 and 3).

Supplementary Figure 2. Example raw data from a biolayer interferometry assay of repressor-DNA binding.

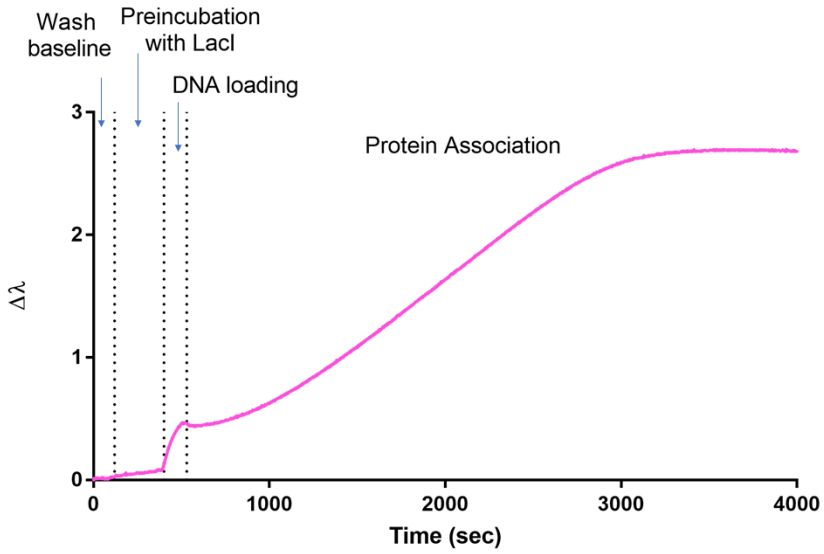

Example raw data from a BLI association experiment, here 6 nM LacI binding to immobilized *lacO*^{1} loaded on the sensor tip from an 80 nM DNA solution. The vertical dashed lines indicate the individual steps of the reaction: Starting from the left of the plot, the tip was first hydrated in buffer and then placed in a tube containing LacI to block any non-specific binding to the tip. Next, the sensor tip was placed in a solution containing biotinylated DNA, followed by a brief wash in buffer only (not visible on this scale and not marked). Finally, the tip with immobilized DNA was placed in a solution containing LacI. Note that the signal arising from repressor binding nonspecifically to the tip is extremely low relative to the signal arising from the repressor-DNA binding step.

Supplementary Figure 3. BLI association and dissociation curves for protein-DNA interactions were multiphasic.

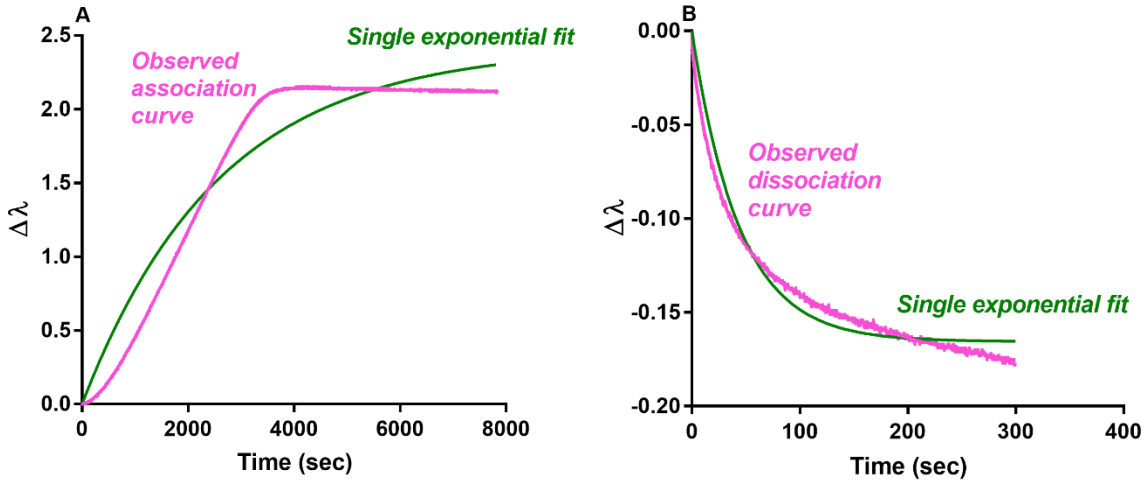

(A) Example association reaction (here, 6 nM LacI binding to immobilized *lacO*^{1} loaded on the tip from an 80 nM solution). The association curve for LacI binding to immobilized DNA (magenta) was not well fit with a single exponential equation (green). Multi-phasic curves were observed for a wide range of protein-DNA binding partners across a wide range of K_d values. We considered whether the sigmoidal curve arose from folding of the hinge helices that is concomitant with DNA binding ((13) and references therein), but sigmoidal character was also observed for a LacI:PurR chimera that does not undergo the large conformational change seen for LacI ((14) and references therein). (B) Dissociation reactions (here, 66 nM LacI binding to immobilized *lacO*^{2} loaded on the tip from an 80 nM solution) could not be fit with single exponential equations, either when dissociation was carried out in buffer or in buffer plus free DNA. One possibility is that biphasic dissociation arose from the combination of specific and nonspecific DNA binding, but attempts to fit association and dissociation curves with biphasic equations did not yield parameters that matched prior determinations of the rate constants that performed with filter binding assays for LacI-DNA (15; 16).

Supplementary Figure 4. The BLI signal at equilibrium correlated with the affinity between LLhF and the DNA operators.

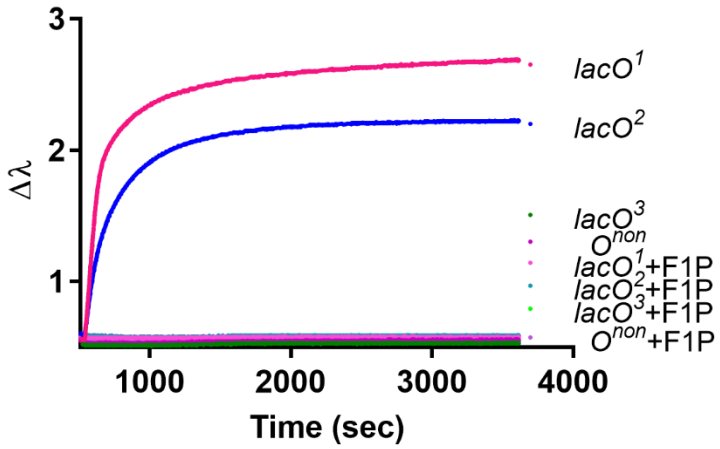

BLI assays of LLhF binding to the *lacO*^{1}, *lacO*^{2}, *lacO*^{3} and *O*^{non} operators in the presence and absence of 1 mM F-1-P inducer. DNA titration curves were collected with the 8-chanel BLI instrument. The concentration of LLhF was 100 nM and the DNA were loaded onto the sensor tip from a solution of 80 nM; the loading step is not shown. Signals for *lacO*^{3}, *O*^{non} and all +F-1-P samples were extremely low in these conditions (bottom of the plot).

Supplementary Figure 5. The midpoint of IPTG-mediated LacI/*lacO*^{1} operator release was independent of a decaying signal.

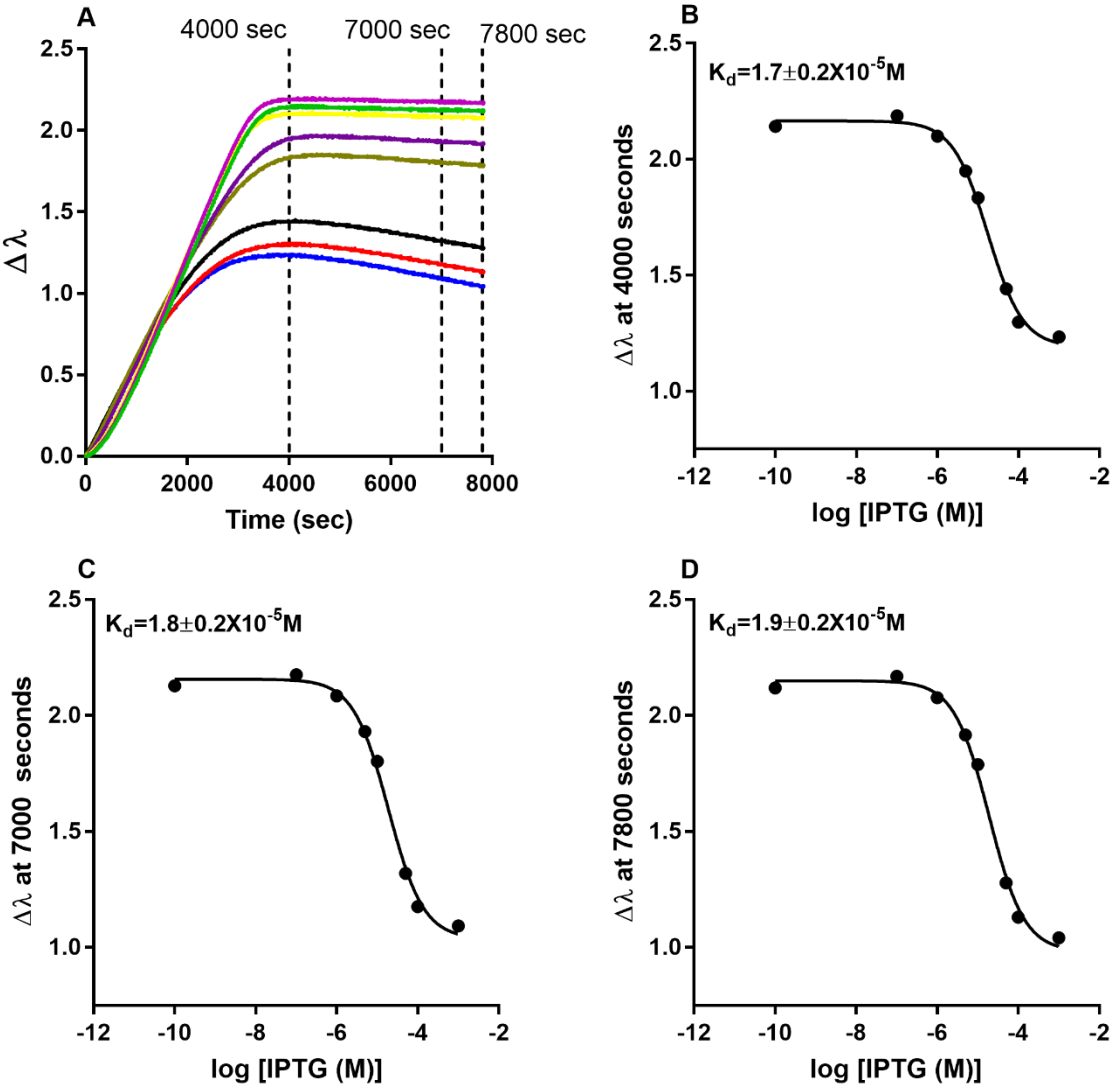

In some BLI assays, the equilibrium "plateaus" of samples decreased instead of remaining constant. We attributed this to protein degradation over the time of the reaction, which might also occur (unobserved) in filter binding assays. (A) The example shown here is for of IPTG-mediated operator release of LacI-*lacO*^{1}. Nevertheless, when different time slices at (B) 4000, (C) 7000 and (D) 7800 seconds were used to generate the Y values and fit with equation 1 (solid lines), the K_d values changed very little. Errors shown are the errors of the fits.

Supplementary Figure 6. Idealized equilibrium and non-equilibrium binding curves.

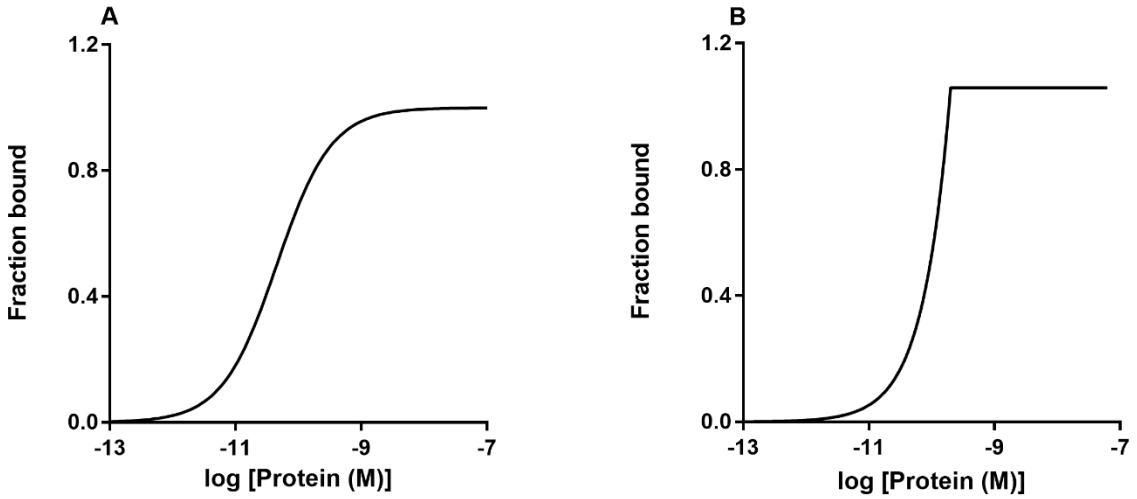

(A) In the equilibrium binding regime ([DNA] < K_d/10), the shape of the binding curve on a semi-log plot is sigmoidal and well-fit to equation 1 (main text). In deriving equation 1, this experimental design allows two simplifying assumptions about the bound and free forms of the DNA and protein that participate in the reaction:

$$Protein_{free} + DNA_{free} \rightleftharpoons Protein\text{-}DNA$$

and for which $K_d = ([Protein]_{free} \bullet [DNA]_{free})/[Protein\text{-}DNA]$

(i) At saturation, essentially all of the DNA is bound and thus the signal at saturation corresponds to the signal of $[DNA]_{total}$. (ii) Since <10% of the protein is bound at any concentration, the concentration of free protein is approximated by the concentration of total protein, which is known by the experimenter.

(B) Under intermediate and stoichiometric binding regime conditions ([DNA] near or greater than K_d), these simplifying assumptions do not apply. The shape of a binding curve on a semi-log plot is not sigmoidal and adequate data fitting requires equation 2 (main text).

Supplementary Figure 7. LacI binding to *lacO*^{2} immobilized to BLI tips was not in the equilibrium regime.

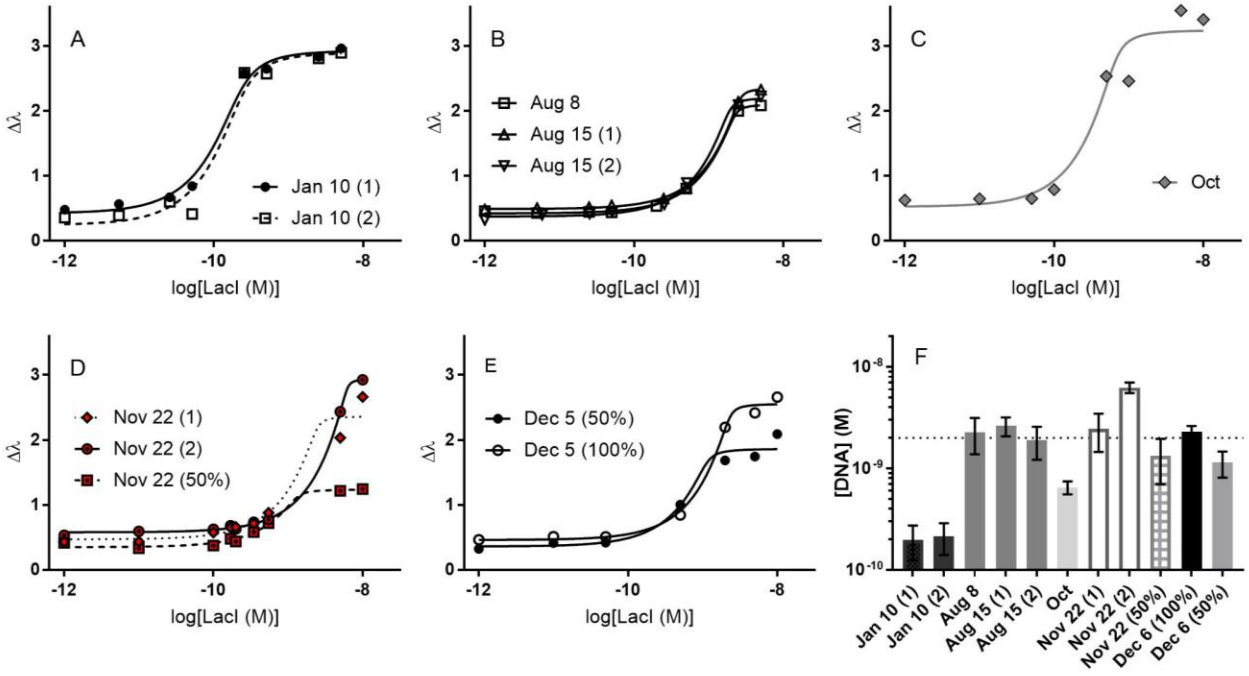

(A-E) Eleven replicates of LacI binding to *lacO*^{2} were fit to equation 2 (main text) via GraphPad prism using a shared fit parameter for K_d and individual fit parameters for DT (total DNA concentration), c, and Y_{max}. The value and fit error for K_d was determined to be 2.7±1.6 x 10^{-11} M, with an upper 95% confidence limit of 7.2x10^{-11} M and an unconstrained lower limit. In panels D and E, the curves labeled "50%" were generated using DNA diluted 1:1 with free biotin prior to immobilization to reduce the total amount of DNA immobilized; the total DNA concentration determined from the fit decreased, as expected. (F) Fit values for the effective concentration of immobilized DNA; these values were near and above the K_d value for LacI binding *lacO*^{2} determined with the filter binding assay (main text Table II). The horizontal dashed line a 2x10^{-9} M is to aid visual inspection. The nonspecific binding event (see Supplementary Figure 2) for some of these replicates used BSA and other replicates used LacI; no significant difference between these conditions was noted.

Supplementary Figure 8. For binding events in the equilibrium regime, changes in the amount of accessible immobilized DNA affected the amplitude but did not affect K_d values.

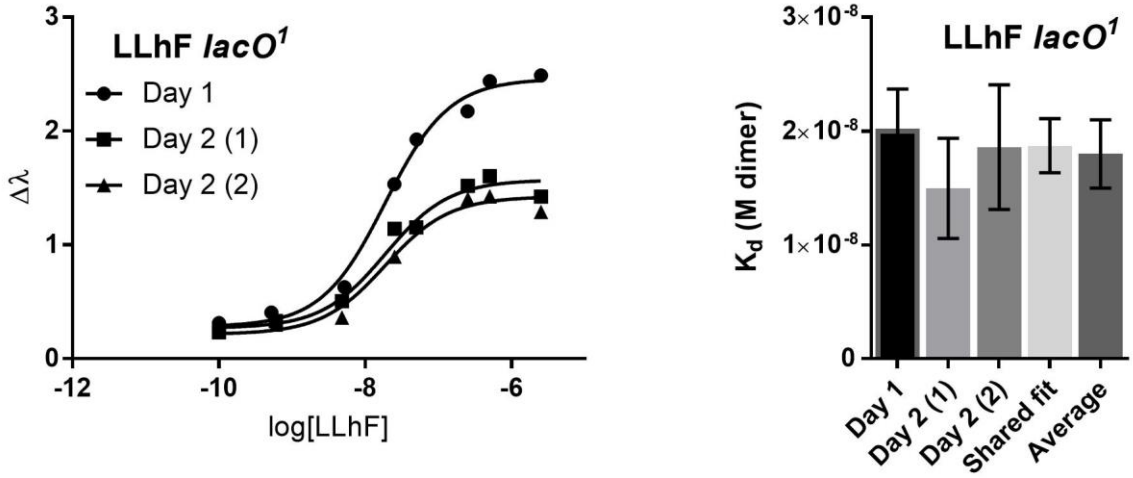

(Left) Replicate binding curves for LLhF binding to *lacO*^{1} showed day-to-day variation in the amplitude of the binding curve, whereas curves generated on the same day generally showed better agreement. This limitation of the BLI assay is also a limitation of the filter binding assay, for which ^{32}P counts differ day-to-day. (Right) K_d values determined with equation 1 (main text) were statistically equivalent for the three curves. This plot shows results of (i-iii) the three individual fits and their fit errors, (iv) a global fit with a shared parameter for K_d ("Shared fit"; error bars are fit error) and independent parameters for c and Y_{max}, and (v) the average and standard deviation of the three individual fits ("Average").

Supplementary Figure 9. LacI at high concentrations ($3x10^{-5}$ M) did not yield reproducible BLI signals.

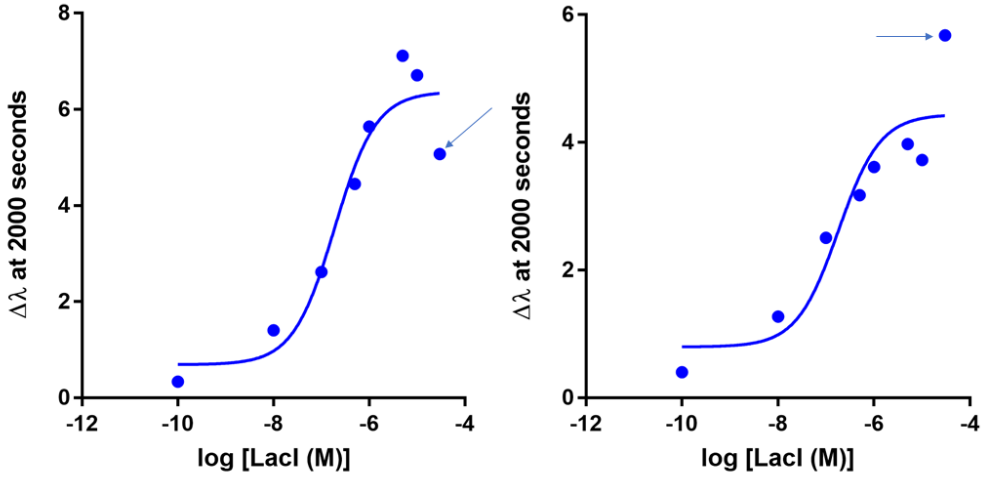

All assays have an upper limit beyond which signal output is not linear. For BLI experiments, high concentrations of LacI (≥ $3x10^{-5}$ M) consistently deviated from the rest of the data (arrows). The examples here are for LacI binding to *lacO*^{3}. For values reported in the main text, these points were excluded from curve fitting. We expect that the upper limit will be protein-dependent and related to the molecular mass of the macromolecule being bound.

Supplementary Figure 10. FruK enzyme activity.

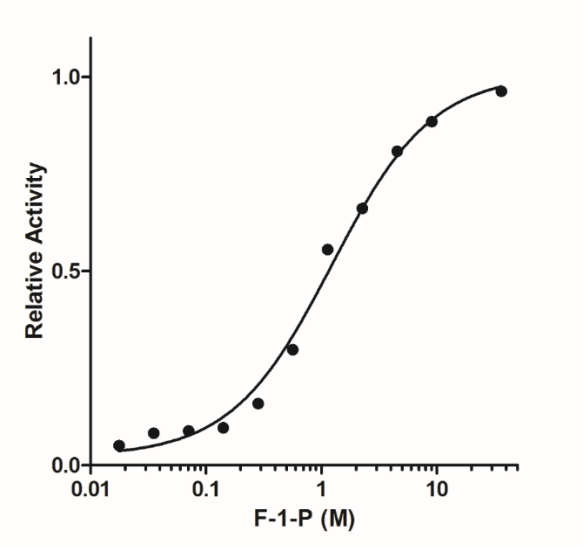

The catalytic activity of FruK was determined as a function of F-1-P concentration as described in the Supplementary Methods. Solid circles represent the measured, initial rates of catalysis, normalized to the maximal value after fitting to the Michaelis-Menten equation. The solid line is the best fit of the Michaelis-Menten equation to the data. From assays of several FruK preparations, we found that K_m for F-1-P was in the range of 0.5-2 mM. In the absence of substrate ATP, no activity was detected.

Supplementary Figure 11. FruK did not bind LacI/*lacO*^{1} or the *fruB-proximal* DNA operator.

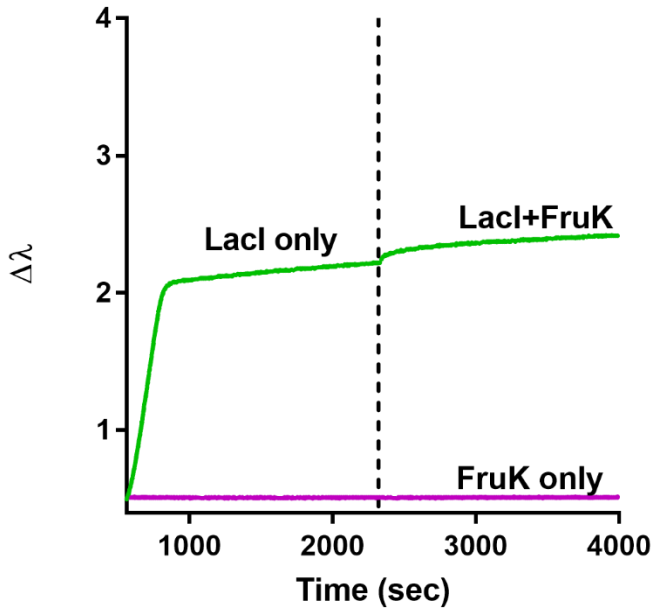

Green: In control experiments for FruK binding, LacI was 30 nM, FruK was 200 nM, and the DNA was biotinylated *lacO*^{1}. The dashed indicates the addition of FruK to the LacI-DNA complex. Purple: Little to no binding was detected when FruK (200 nM) was incubated with the immobilized FruR operator *fruB-proximal*. In both experiments, DNA was loaded onto the BLI sensor tip from a solution of 80 nM; for simplicity in the graph, the loading step is not shown.

Supplementary References

All references below are also cited in the main text.

1. Swint-Kruse L, Zhan H, Matthews KS (2005) Integrated insights from simulation, experiment, and mutational analysis yield new details of LacI function. Biochemistry 44:11201-11213.
2. Gardner JA, Matthews KS (1990) Characterization of two mutant lactose repressor proteins containing single tryptophans. J Biol Chem 265:21061-21067.
3. Sommer H, Lu P (1976) Lac Repressor. Fluorescence of the two tryptophans. J Biol Chem 251:3774-3779.
4. Swint-Kruse L, Matthews KS (2004) Thermodynamics, protein modification, and molecular dynamics in characterizing lactose repressor protein: strategies for complex analyses of protein structure-function. Methods Enzymol 379:188-209.
5. Meinhardt S, Manley MW, Becker NA, Hessman JA, Maher LJ, Swint-Kruse L (2012) Novel insights from hybrid LacI/GalR proteins: family-wide functional attributes and biologically significant variation in transcription repression. Nucleic Acids Research 40:11139-11154.
6. Swint-Kruse L, Elam CR, Lin JW, Wycuff DR, Shive Matthews K (2001) Plasticity of quaternary structure: twenty-two ways to form a LacI dimer. Protein Sci 10:262-276.
7. Wycuff DR, Matthews KS (2000) Generation of an Ara-C-*ara*BAD promoter-regulated T7 expression system. Analytical Biochemistry 277:67-73.
8. Veiga-da-Cunha M, Hoyoux A, Van Schaftingen E (2000) Overexpression and purification of fructose-1-phosphate kinase from Escherichia coli: application to the assay of fructose 1-phosphate. Protein Expr Purif 19:48-52.
9. Ferenci T, Kornberg HL (1973) The utilization of fructose by Escherichia coli. Properties of a mutant defective in fructose 1-phosphate kinase activity. Biochem J 132:341-347.
10. Fenton AW, Alontaga AY (2009) The impact of ions on allosteric functions in human liver pyruvate kinase. Methods Enzymol 466:83-107.
11. Singh D, Fairlamb MS, Harrison KS, Weeramange C, Meinhardt S, Tungtur S, Rau BF, Hefty PS, Fenton AW, Swint-Kruse L (2017) Protein-protein interactions with fructose-1-kinase alter function of the central *Escherichia coli* transcription regulator, Cra. bioRxiv 10.1101/201277.
12. Ramseier TM, Negre D, Cortay JC, Scarabel M, Cozzone AJ, Saier MH, Jr. (1993) In vitro binding of the pleiotropic transcriptional regulatory protein, FruR, to the fru, pps, ace, pts and icd operons of Escherichia coli and Salmonella typhimurium. J Mol Biol 234:28-44.
13. Taraban M, Zhan H, Whitten AE, Langley DB, Matthews KS, Swint-Kruse L, Trewhella J (2008) Ligand-induced Conformational Changes and Conformational Dynamics in the Solution Structure of the Lactose Repressor Protein. J Mol Biol 376:466-481.
14. Zhan H, Taraban M, Trewhella J, Swint-Kruse L (2008) Subdividing repressor function: DNA binding affinity, selectivity, and allostery can be altered by amino acid substitution of nonconserved residues in a LacI/GalR homologue. Biochemistry 47:8058-8069.
15. Whitson PA, Matthews KS (1986) Dissociation of the lactose repressor-operator DNA complex: effects of size and sequence context of operator-containing DNA. Biochemistry 25:3845-3852.
16. Riggs AD, Bourgeois S, Cohn M (1970) The lac repressor-operator interaction. 3. Kinetic studies. J Mol Biol 53:401-417.